© 2000 The Chemical Society of Japan Bull. Chem. Soc. Jpn., 73, 2297—2303 (2000)

Structural Characteristics of *S*-Bridged Trinuclear Complexes $[\{Pd(terpy)\}_2\{Pd(aet)_2\}]^{4+}$ (terpy = 2,2′ : 6′,2″-Terpyridine, aet = 2-Aminoethanethiolate): Effects of Counter Anions and Solvent on Intra- and Intermolecular Stacking Arrangements

Yasunori Yamada,* Kiyoshi Fujisawa, and Ken-ichi Okamoto*

Department of Chemistry, University of Tsukuba, Tsukuba, Ibaraki 305-8571

(Received April 17, 2000)

S-bridged trinuclear Pd(II) complexes, $[\{Pd(terpy)\}_2\{Pd(aet)_2\}]X_4\cdot n$Solv (terpy = 2,2′ : 6′,2″-terpyridine, aet = 2-aminoethanethiolate; X = PF_6^-, *n* = 2, Solv = CH_3CN (**1**); X = BF_4^-, *n* = 0.5, Solv = H_2O (**2**); X = BF_4^-, *n* = 0 (**3**); 2X = SiF_6^{2-}, *n* = 6, Solv = H_2O (**4**)), were obtained by the reactions of $[Pd(aet)_2]$ (aet = 2-aminoethanethiolate) with $[Pd(NO_3)(terpy)]^+$ (terpy = 2,2′ : 6′,2″-terpyridine) using some kinds of counter anions and solvents. The molecules of **1**—**4**, whose structures were determined by X-ray crystallography, contain two {Pd(terpy)} moieties bridged by one $[Pd(aet)_2]$ unit. Although the molecular structures of these complexes are similar to each other, they have significantly different intermolecular structures from each other. While **1** and **2** take monomeric structures, **3** and **4** exist as polymeric forms. These structural features also reflect their diffuse reflection spectra.

Square-planar d^8 metal complexes with aromatic diimine ligands, such as 2,2′-bipyridine (bpy), 1,10-phenanthroline (phen), and their derivatives, sometimes take stacking structures due to π–π interactions of the pyridyl rings in the crystalline state.[1—5] Such types of complexes exhibit specific spectral, structural, and electrochemical properties.[1,2,5—8] On the basis of these facts, numerous types of complexes have been synthesized by using various aromatic diimine ligands, and characterized by some chemical methods.[1—14] However, investigations on such π–π stacking were almost limited to mononuclear complexes. On the other hand, polynuclear complexes with intramolecular stacking arrangements by plural {M(diimine)} (M = Pd^{II}, Pt^{II}, or Au^{III}) moieties are of current interest, since they can provide significant information on linear-chain structures and/or metal–metal interactions. There are few examples for these types of polynuclear complexes, except for the complexes bridged by simple anion ligands or intricate organic ligands.[9,10,15—19] Recently, we have found, however, that a simple reaction between $[Pd(aet)_2]$ (aet = 2-aminoethanethiolate) including two donating S atoms and $[Pd(NO_3)_2(bpy)]$ gave an *S*-bridged tetranuclear complex, $[\{Pd(bpy)\}_2\{Pd(aet)_2\}_2]^{4+}$, in which two {Pd(bpy)} moieties are situated in an intramolecular stacking arrangement due to π–π interactions.[20] Furthermore, this complex takes a dimeric form due to an intermolecular interaction in the crystalline state. It is generally known that the size of the π-electronic system or steric factor of the diimine ligand affects the crystal structure of the complex, and that the stacking modes are also influenced by counter anions and/or solvent co-existing in the crystals.[3] Taking these facts into consideration, diversity of the stacking modes is expected for a similar-type trinuclear complex, $[\{Pd(terpy)_2\{Pd(aet)_2\}\}^{4+}$ (terpy = 2,2′ : 6′,2″-terpyridine), which is considered to be obtained by the reaction of $[Pd(aet)_2]$ with $[Pd(NO_3)(terpy)]^+$, owing to an expansion of the π-electronic system in a terpy skeleton and/or flexibility for the configuration based on a bridging $[Pd(aet)_2]$ unit. Although the corresponding Pt(II) complex, $[\{Pt(terpy)\}_2\{Pt(aet)_2\}]^{4+}$, has been previously reported,[21] the diversity in the structure, depending on counter anion and/or solvent of crystallization, remains unclear. In the present paper, we report on the synthesis of the trinuclear complexes, $[\{Pd(terpy)_2\{Pd(aet)_2\}\}X_4\cdot n$Solv (X = PF_6^-, *n* = 2, Solv = CH_3CN (**1**); X = BF_4^-, *n* = 0.5, Solv = H_2O (**2**); X = BF_4^-, *n* = 0 (**3**); 2X = SiF_6^{2-}, *n* = 6, Solv = H_2O (**4**)) and their crystal structures. The diffuse reflection spectral features of these complexes are also discussed in relation to their crystal structures.

Experimental

Materials. Na_2PdCl_4, 2,2′ : 6′,2″-terpyridine, and 2-aminoethanethiolate hydrochloride were purchased from Tanaka Rare Metal Industries Ltd., Aldrich Chemical Co., Inc., and Tokyo Chemical Co., Ltd., respectively. $NaBF_4$, NH_4PF_6, and $(NH_4)_2SiF_6$ were obtained from Wako Pure Chemical Ind. Co., Ltd., Aldrich Chemical Co., Inc., and Soekawa Chemical Co., Ltd, respectively. $[Pd(NO_3)(terpy)]NO_3$ and $[Pd(aet)_2]$ were prepared by modified methods from the literature.[22—24] The other chemicals were obtained from Wako Pure Chemical Ind. Co., Ltd., or Tokyo Chemical Co., Ltd. All of the chemicals were of reagent grade and used without further purification.

Preparation of Complexes. [{Pd(terpy)}$_2${Pd(aet)$_2$}]-(PF$_6$)$_4$·2CH$_3$CN (1). To a suspension containing 0.13 g (0.5 mmol) of [Pd(aet)$_2$] in 50 cm^3 of water was added 0.50 g (1.0 mmol) of [Pd(NO$_3$)(terpy)]NO$_3$. The mixture was stirred at 85 °C for 24 h, whereupon the mixture became an orange solution. After cooling to room temperature, 1.63 g (10 mmol) of NH$_4$PF$_6$ was added to the above-mentioned orange solution. The resulting yellow microcrystals of **1** were collected by filtration, and recrystallized by vapor diffusion of diethyl ether into an acetonitrile solution. A well-formed crystal of **1** was used for an X-ray structural analysis. Yield: 0.61 g (76%). Calcd for [{Pd(terpy)}$_2${Pd(aet)$_2$}]-(PF$_6$)$_4$·2CH$_3$CN = $C_{38}H_{40}N_{10}F_{24}P_4S_3Pd_3$: C, 28.52; H, 2.52; N, 8.75%. Found: C, 27.95; H, 2.46; N, 8.32%.

[{Pd(terpy)}$_2${Pd(aet)$_2$}](BF$_4$)$_4$·0.5H$_2$O (2). To an orange solution obtained by the same procedure as in the synthesis of **1** at 50 °C was added 50 cm^3 of water and 1.10 g (10 mmol) of NaBF$_4$. After removing unreacted materials by filtration, the filtrate was allowed to stand at room temperature for several days. The resulting yellow crystals were collected by filtration. A well-formed crystal of **2** was used for an X-ray structural analysis. Thermogravimetric analyses of **2** exhibit a gradual decrease of 1.0%, corresponding to a half water of crystallization from room temperature to 110 °C, and no decrease from 110 to 250 °C. Yield: 0.47 g (72%). Calcd for [{Pd(terpy)}$_2${Pd(aet)$_2$}](BF$_4$)$_4$·0.5H$_2$O = $C_{34}H_{35}B_4N_8O_{0.5}F_{16}S_2Pd_3$: C, 31.55; H, 2.73; N, 8.66%. Found: C, 30.63; H, 2.69; N, 8.44%.

[{Pd(terpy)}$_2${Pd(aet)$_2$}](BF$_4$)$_4$ (3). To an orange solution obtained by the same procedure as in the synthesis of **1** in a higher concentration at 50 °C was added 0.55 g (5 mmol) of NaBF$_4$. After removing unreacted materials by filtration, the filtrate was allowed to stand at room temperature overnight. The resulting red-orange crystals with quite different shapes and colors from those of the crystals of **2** were collected by filtration. A well-formed crystal of **3** was used for an X-ray structural analysis. Thermogravimetric analyses exhibited a decrease of less than 0.05% from room temperature to 250 °C. Yield: 0.42 g (65%). By standing the filtrate at room temperature for several days, yellow crystals of **2** were also obtained. Yield: 0.16 g (25%). Calcd for [{Pd(terpy)}$_2${Pd(aet)$_2$}](BF$_4$)$_4$ = $C_{34}H_{34}B_4N_8F_{16}S_2Pd_3$: C, 31.77; H, 2.67; N, 8.72%. Found: C, 31.17; H, 2.64; N, 8.55%.

[{Pd(terpy)}$_2${Pd(aet)$_2$}](SiF$_6$)$_2$·6H$_2$O (4). To an orange solution obtained by the same procedure as in the synthesis of **1** at 50 °C was added 1.78 g (10 mmol) of (NH$_4$)$_2$SiF$_6$. After removing unreacted materials by filtration, the filtrate was allowed to stand at room temperature for a few days. The resulting red-orange crystals were collected by filtration. A well-formed crystal of **4** was used for an X-ray structural analysis. Yield: 0.53 g (80%). Calcd for [{Pd(terpy)}$_2${Pd(aet)$_2$}](SiF$_6$)$_2$·6H$_2$O = $C_{34}H_{46}N_8O_6F_{12}Si_2S_2Pd_3$: C, 30.69; H, 3.48; N, 8.42%. Found: C, 30.46; H, 3.48; N, 8.15%.

Measurement. Diffuse reflection spectra were recorded with a JASCO Ubest V-570 spectrophotometer at room temperature. Thermogravimetric analyses were performed with a Seiko Exstar6000 thermogravimeter. Elemental analyses (C, H, N) were performed by the Analysis Center of the University of Tsukuba.

Crystallography. The unit-cell parameters and intensity data for **1**—**4** were obtained on a Rigaku RASA-7S four-circle diffractometer with graphite-monochromatized Mo $K\alpha$ radiation. The unit-cell parameters were determined by a least-square refinement of 25 reflections with 2θ values of $10° < 2\theta < 30°$. The crystal data and experimental parameters are listed in Table 1. The intensity data were collected by the ω–2θ scan technique, and corrected for Lorentz and polarization. An empirical absorption correction based on a series of Ψ scans was applied, except for **1**. Independent reflections with $I_0 > 2\sigma(I_0)$ were used for structure determinations. The positions of the Pd and some atoms were determined by a direct method. Difference Fourier maps based on these atomic positions revealed the remaining non-hydrogen atoms. The structures were refined by a full-matrix least-squares refinement on F of the positional parameters and the anisotropic thermal parameters of the non-hydrogen atoms in **1**—**4**. The hydrogen atoms on

Table 1. Crystal Data of [{Pd(terpy)}$_2${Pd(aet)$_2$}](PF$_6$)$_4$·2CH$_3$CN (**1**), [{Pd(terpy)}$_2${Pd(aet)$_2$}](BF$_4$)$_4$·0.5H$_2$O (**2**), [{Pd(terpy)}$_2${Pd(aet)$_2$}](BF$_4$)$_4$ (**3**), and [{Pd(terpy)}$_2${Pd(aet)$_2$}](SiF$_6$)$_2$·6H$_2$O (**4**)

	1	**2**	**3**	**4**
Formula	$C_{38}H_{40}N_{10}F_{24}P_4S_3Pd_3$	$C_{17}H_{17.50}B_2N_4O_{0.25}F_8SPd_{1.50}$	$C_{34}H_{34}B_4N_8F_{16}S_2Pd_3$	$C_{17}H_{23}N_4O_3F_6SiSPd_{1.5}$
Fw	1599.98	647.12	1285.23	665.13
Cryst dimens / mm	0.28 × 0.23 × 0.18	0.35 × 0.30 × 0.25	0.35 × 0.25 × 0.20	0.40 × 0.40 × 0.40
Space group	$P\bar{1}$	$I4_1/a$	$P2_1/n$	$C2/c$
a / Å	13.570(6)	16.315(2)	15.570(2)	20.866(3)
b / Å	18.249(8)		13.276(3)	19.926(2)
c / Å	11.651(4)	34.446(5)	22.364(2)	15.482(3)
α / deg	97.74(3)			
β / deg	94.46(3)		107.87(1)	132.115(6)
γ / deg	106.19(3)			
V /Å^3	2725(1)	9168(2)	4399(1)	4775(1)
Z	2	16	4	8
D_{calcd} / g cm^{-3}	1.949	1.875	1.940	1.850
μ / cm^{-1}	12.98	13.60	14.16	13.54
Transm factor	—	0.93—1.00	0.79—1.00	0.71—0.99
Scan type	ω–2θ	ω–2θ	ω–2θ	ω–2θ
2θ range / deg	55.0	55.0	55.0	55.1
No. of reflcns measd	11828	5636	10467	5658
No. of reflcns used	7408	3304	4797	4610
No. of variables used	730	339	604	335
R (R_w)	0.054 (0.069)	0.038 (0.047)	0.054 (0.062)	0.042 (0.065)

the ligands were fixed by both geometrical and thermal constraints (C–H = N–H = 0.95 Å and $U = 1.3U$ (C, N)). All of the calculations were performed on an Indigo II computer using teXsan.[25] The final atomic positional parameters are deposited in Tables S1—S12.[26] Crystallographic data have been deposited at the CCDC, 12 Union Road, Cambridge CB2 1EZ, UK and copies can be obtained on request, free of charge, by quoting the publication citation and the deposition numbers 146617—146620.

Results and Discussion

Syntheses. A square-planar mononuclear metalloligand, $[Pd(aet)_2]$, including two donating S atoms, reacted with two molar equivalents of $[Pd(NO_3)(terpy)]^+$ to form an *S*-bridged trinuclear structural $[\{Pd(terpy)\}_2\{Pd(aet)_2\}]^{4+}$ via substitution of the nitrate anion of the latter complex with S atoms in the former complex. A treatment of the complex cation with hexafluorophosphate, tetrafluoroborate, and hexafluorosilicate anions in water gave three types of complex salts. Furthermore, two different kinds of crystals, whose shapes and colors were distinctly different from each other, were obtained for tetrafluoroborate salts, depending on the concentration of the complex in the reaction mixtures. These four crystals are structurally distinguishable from each other, as mentioned below. In crystals of the hexafluorophosphate salts of **1**, complex cations, in which two π-electronic systems of the terpy skeletons interact with each other, exist in monomeric forms. Although the tetrafluoroborate salt of **2**, including a half water molecule, also takes a monomeric structure, the intramolecular stacking arrangement is partially different from that of **1**. In other crystals of the tetrafluoroborate salts of **3** without water of crystallization, on the other hand, the complex cations are situated in an intermolecular π–π stacking arrangement. A half water molecule for **2** and no water of crystallization for **3** are supported by the results of thermogravimetric analyses, which indicate that the crystals of **2** contain about 1.0% water, and that the crystals of **3** contain less than 0.05% water. Further, the complex cations in the crystals of the hexafluorosilicate salts of **4** build up linear-chain-like structures. These structural differences in the above-mentioned four crystals reflect their spectral behavior.

Crystal Structure of $[\{Pd(terpy)\}_2\{Pd(aet)_2\}](PF_6)_4\cdot 2CH_3CN$ (1). An X-ray structural analysis for **1** revealed the presence of a discrete tetravalent complex cation, four hexafluorophosphate anions, and two acetonitrile molecules. A perspective drawing of the complex cation of **1** is given in Fig. 1, and its selected bond distances and angles are listed in Table 2 in comparison with those of **2**—**4**. As shown in Fig. 1, **1** contains two square-planar {Pd(terpy)} moieties and one $[Pd(aet)_2]$ unit to form the *S*-bridged trinuclear structure. Each of two Pd atoms in the {Pd(terpy)} moieties is bridged by one S atom from the $[Pd(aet)_2]$ unit to allow two {Pd(terpy)} planes to be partially overlapped. Namely, the N(2), N(3), C(10), C(12), C(14), and C(15) atoms in one {Pd(terpy)} moiety are significantly close to the C(30), N(6), C(29), C(27), C(25), and N(5) atoms in the other {Pd(terpy)} moiety, respectively (N(2)–C(30) = 3.597(9), N(3)–N(6) = 3.376(8), C(10)–C(29) = 3.49(1), C(12)–C(27) = 3.58(1), C(14)–C(25) = 3.43(1), and C(15)–N(5) = 3.579(9) Å). The interplane distance and the angle between the least-squares planes of the two {Pd(terpy)} moieties are 3.399 Å and 1.08°, respectively, indicating that two {Pd(terpy)} moieties in the complex cation can considerably interact with each other. Although these structural features are similar to those of the complex cation, $[\{Pd(bpy)_2\}\{Pd(aet)_2\}_2]^{4+}$,[20] the intermetal distance (Pd(1)–Pd(2) = 4.0973(7) Å) between two Pd atoms in two square-planar moieties is significantly longer than the corresponding distance (3.3149(4) Å) in $[\{Pd(bpy)_2\}\{Pd(aet)_2\}_2]^{4+}$. This implies that two Pd atoms in the {Pd(terpy)} moieties do not participate in the stacking arrangement. It is notable that the Pd–S–Pd bridging angles (av 110.65(7)°) are significantly different from those (av 115.50(4)°) in $[\{Pd(bpy)_2\}\{Pd(aet)_2\}_2]^{4+}$, in which two {Pd(bpy)} moieties are bridged by two $[Pd(aet)_2]$ units. As shown in Fig. 2, one vacant axial site of each of two Pd atoms in the {Pd(terpy)} moieties seems to be occupied by a fluorine atom of the hexafluorophosphate anion (Pd–F = av 3.166(8) Å). This indicates an interaction between the Pd and F atoms, resulting in the monomeric structure of **1**.

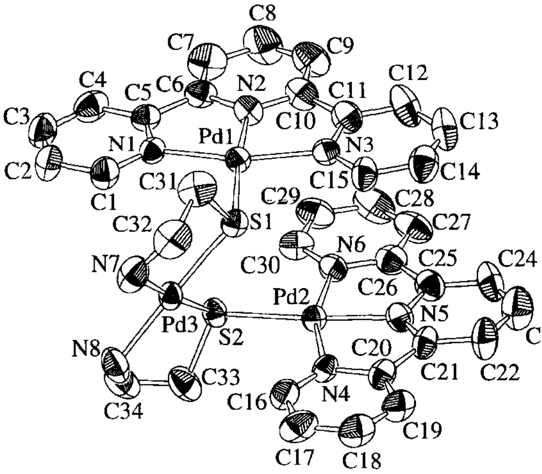

Fig. 1. Perspective view of $[\{Pd(terpy)\}_2\{Pd(aet)_2\}](PF_6)_4\cdot 2CH_3CN$ (**1**) with the atomic labeling scheme.

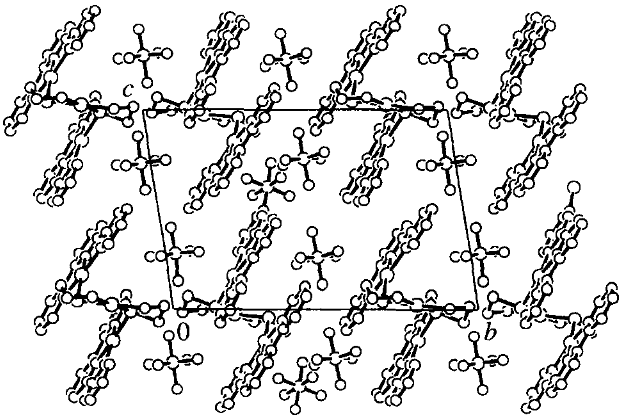

Fig. 2. Projection of crystal packing for $[\{Pd(terpy)\}_2\{Pd(aet)_2\}](PF_6)_4\cdot 2CH_3CN$ (**1**) viewed along *a* axis.

Table 2. Selected Bond Distances (Å) and Angles (deg) of [{Pd(terpy)}$_2${Pd(aet)$_2$}](PF$_6$)$_4$·2CH$_3$CN (**1**), [{Pd(terpy)}$_2${Pd(aet)$_2$}](BF$_4$)$_4$·0.5H$_2$O (**2**), [{Pd(terpy)}$_2${Pd(aet)$_2$}](BF$_4$)$_4$ (**3**), and [{Pd(terpy)}$_2${Pd(aet)$_2$}](SiF$_6$)$_2$·6H$_2$O (**4**)

		1	**2**	**3**	**4**
Pd(1)–S(1)		2.296(1)	2.298(1)	2.295(2)	2.290(1)
Pd(1)–N(1)		2.050(6)	2.035(4)	2.032(7)	2.044(5)
Pd(1)–N(2)		1.967(4)	1.953(4)	1.980(7)	1.944(4)
Pd(1)–N(3)		2.038(6)	2.045(4)	2.040(7)	2.044(4)
Pd(2)–S(2)		2.299(2)		2.294(2)	
Pd(2)–N(4)		2.059(4)		2.052(8)	
Pd(2)–N(5)		1.958(6)		1.958(8)	
Pd(2)–N(6)		2.047(4)		2.038(7)	
Pd(3)–S(1)	(Pd(2)–S(1))	2.256(2)	2.259(1)	2.252(2)	2.265(1)
Pd(3)–S(2)	(Pd(2)–S(1*)	2.259(2)	2.259(1)	2.257(3)	2.265(1)
Pd(3)–N(7)	(Pd(2)–N(4))	2.099(6)	2.075(4)	2.069(9)	2.077(3)
Pd(3)–N(8)	(Pd(2)–N(4*))	2.107(7)	2.075(4)	2.070(6)	2.077(3)
S(1)–Pd(1)–N(1)		104.5(1)	95.3(1)	95.6(2)	95.5(1)
S(1)–Pd(1)–N(2)		173.8(2)	172.2(1)	175.1(2)	174.8(1)
S(1)–Pd(1)–N(3)		94.6(1)	104.4(1)	103.5(2)	103.4(1)
N(1)–Pd(1)–N(2)		80.5(2)	80.2(2)	80.6(3)	80.5(2)
N(1)–Pd(1)–N(3)		160.9(2)	160.3(1)	160.9(3)	161.1(1)
N(2)–Pd(1)–N(3)		80.4(2)	80.2(2)	80.3(3)	80.6(2)
S(2)–Pd(2)–N(4)		104.2(2)		94.1(2)	
S(2)–Pd(2)–N(5)		175.2(2)		174.6(2)	
S(2)–Pd(2)–N(6)		95.0(2)		104.5(2)	
N(4)–Pd(2)–N(5)		80.0(2)		80.5(3)	
N(4)–Pd(2)–N(6)		160.8(2)		161.4(3)	
N(5)–Pd(2)–N(6)		80.8(2)		81.0(3)	
S(1)–Pd(3)–S(2)	(S(1)–Pd(2)–S(1*))	90.55(6)	94.84(6)	95.78(8)	99.28(5)
S(1)–Pd(3)–N(7)	(S(1)–Pd(2)–N(4))	85.5(2)	85.4(1)	86.2(2)	85.14(10)
S(1)–Pd(3)–N(8)	(S(1)–Pd(2)–N(4*))	176.2(2)	176.0(1)	171.2(2)	172.4(1)
S(2)–Pd(3)–N(7)	(S(1*)–Pd(2)–N(4))	176.0(2)	176.0(1)	170.4(2)	172.4(1)
S(2)–Pd(3)–N(8)	(S(1*)–Pd(2)–N(4*))	85.8(2)	85.4(1)	85.5(2)	85.14(10)
N(7)–Pd(3)–N(8)	(N(4)–Pd(2)–N(4*))	98.1(2)	94.6(2)	94.0(3)	91.2(2)
Pd(1)–S(1)–Pd(3)	(Pd(1)–S(1)–Pd(2))	110.52(7)	117.01(5)	116.9(1)	116.75(6)
Pd(2)–S(2)–Pd(3)		110.78(7)		120.31(10)	

Crystal Structure of [{Pd(terpy)}$_2${Pd(aet)$_2$}](BF$_4$)$_4$·0.5H$_2$O (2). As shown in Fig. 3, although the structure of **2** is quite similar to that of **1**, two {Pd(terpy)} planes in **2** are overlapped by a different manner from **1**. Namely, the Pd(1), C(1), C(4), and C(6) atoms in one {Pd(terpy)} moiety are significantly close to the Pd(1*), C(11*), C(9*), and C(6*) atoms in the other {Pd(terpy)} moiety, respectively (Pd(1)–Pd(1*) = 3.3551(8), C(1)–C(11*) = 3.499(7), C(4)–C(9*) = 3.589(8), and C(6) – C(6*) = 3.54(1) Å). Further, the interplane distance and angle between the least-squares planes of the two {Pd(terpy)} moieties are 3.455 Å and 1.27°, respectively. The intermetal distance (Pd(1)–Pd(1*) = 3.374(1) Å) between two Pd atoms in the two square-planar moieties is more approached than the corresponding distances in **1**, but is relatively longer than that (3.3149(4) Å) in [{Pd(bpy)$_2$}{Pd(aet)$_2$}$_2$]$^{4+}$.[20] On the other hand, the Pd–S–Pd bridging angle (117.01(5)°) is considerably different from those (av 110.65(7)°) in **1**. This reflects the difference in the stacking arrangement between **1** and **2**. Similarly to the case of **1**, as shown in Fig. 4, one vacant axial site of each of two Pd atoms in the {Pd(terpy)} moieties is occupied by a fluorine atom of the tetrafluoroborate anion (Pd–F = 3.194(5) Å). This results in the monomeric structure of **2**, as in the case of **1**.

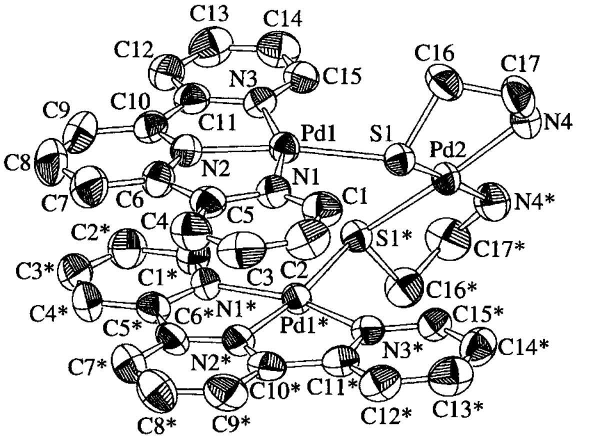

Fig. 3. Perspective view of [{Pd(terpy)}$_2${Pd(aet)$_2$}](BF$_4$)$_4$·0.5H$_2$O (**2**) with the atomic labeling scheme.

Crystal Structure of [{Pd(terpy)}$_2${Pd(aet)$_2$}](BF$_4$)$_4$ (3). Contrary to the crystal of **2** with the same counter anions, there is no water of crystallization in the crystal of **3**. However, the intramolecular structure of **3** is almost identical with that of **2** (Table 2). Namely, two {Pd(terpy)} planes

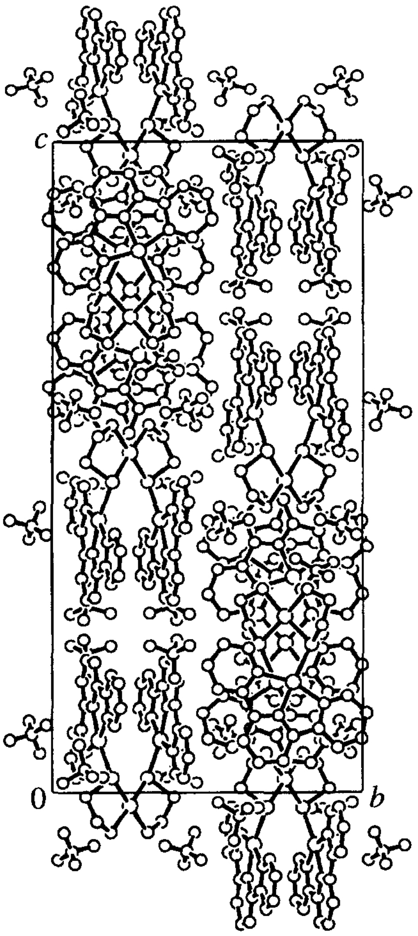

Fig. 4. Projection of crystal packing for [{Pd(terpy)}$_2${Pd(aet)$_2$}](BF$_4$)$_4$·0.5H$_2$O (**2**) viewed along *a* axis.

are considerably overlapped and the interplane distance and angle between the least squares planes of two {Pd(terpy)} moieties are 3.405 Å and 4.47°, respectively. This indicates that the two {Pd(terpy)} moieties in the complex cation can considerably interact with each other. On the other hand, the Pd–S–Pd bridging angles (av 118.6(1)°) are almost identical with that (117.01(5)°) of **2**, but significantly different from those (av 110.65(7)°) of **1**. In contrast to **2**, one vacant axial site of one Pd atom in the {Pd(terpy)} moiety is occupied by a fluorine atom of the tetrafluoroborate anion (Pd–F = av 3.090(7) Å) (Fig. 5). Furthermore, one vacant axial site of another Pd atom in the {Pd(terpy)} moiety is not occupied by a counter anion. As a result, one {Pd(terpy)} moiety (*A*) allows partial stacking with one {Pd(terpy)} moiety in an adjacent complex cation (*B*); that is, the N(6), C(22), and C(24) atoms in one complex cation *A* are close to the C(24), C(28), and C(26) atoms in the adjacent complex cation *B*, respectively (N(6*A*)–C(24*B*) = 3.51(1), C(22*A*)–C(28*B*) = 3.53(1), and C(24*A*)–C(26*B*) = 3.45(1) Å). In addition, other types of π–π interactions are considered to exist; that is, the C(16) and C(17) atoms in complex cation *A* are close to the C(18) and C(17) atoms in another complex cation (*C*), respectively (C(16*A*)–C(18*C*) = 3.536(9) and C(17*A*)–C(17*C*) = 3.48(1) Å). Accordingly, there are two kinds of π–π interactions in the crystal of **3**. These two intermolecular stacking modes contribute to the packing mode of **3**.

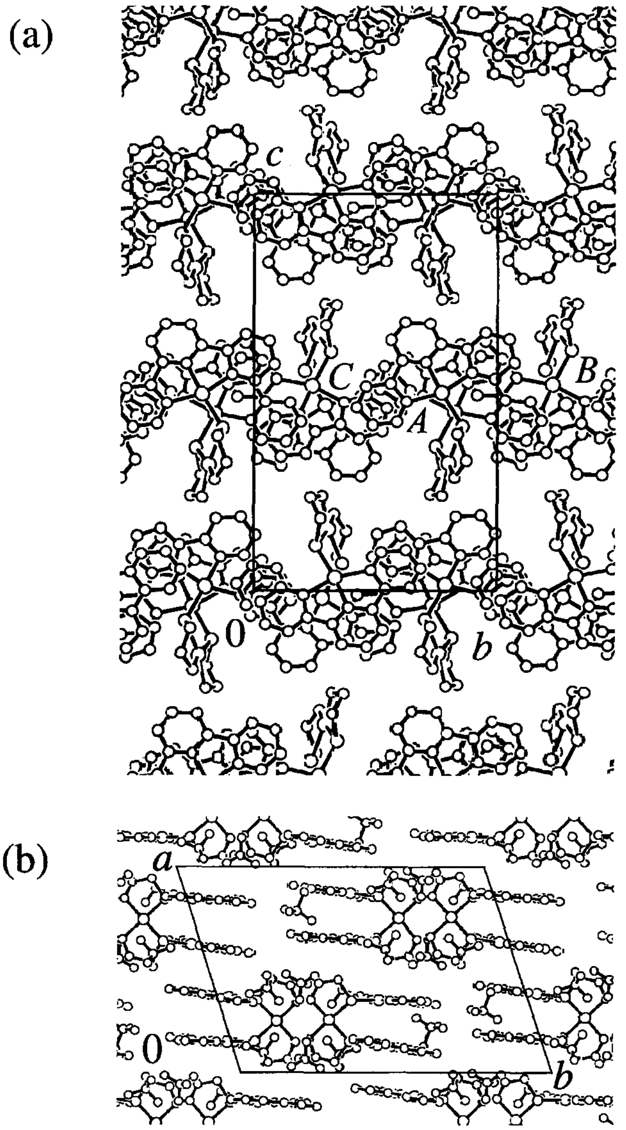

Fig. 5. Projection of crystal packing for [{Pd(terpy)}$_2${Pd(aet)$_2$}](BF$_4$)$_4$ (**3**) (a) viewed along *a* axis and (b) viewed along *c* axis.

Crystal Structure of [{Pd(terpy)}$_2${Pd(aet)$_2$}](SiF$_6$)$_2$·6H$_2$O (4). The intramolecular structure of **4** is almost identical with that of **3**. On the other hand, the intermolecular structure of the former is significantly distinct from that of the latter. Regarding the intramolecular structure, the interplane distance and angle between the least-squares planes of the two {Pd(terpy)} moieties are 3.417 Å and 0.21°, respectively. This is similar to the case of **2** and **3**, indicating that the two {Pd(terpy)} moieties in the complex cation can considerably interact with each other. The Pd–S–Pd bridging angle (116.75(4)°) is almost identical with those in **2** (117.01(5)°) and **3** (av 118.6(1)°), but distinct from those (av 110.65(7)°) of **1**. In contrast to **1**, **2**, and **3**, no counter anions occupy the vacant axial sites of the Pd atoms in the {Pd(terpy)} moieties (Fig. 6). This results in that **4** exists in a linear-chain-like

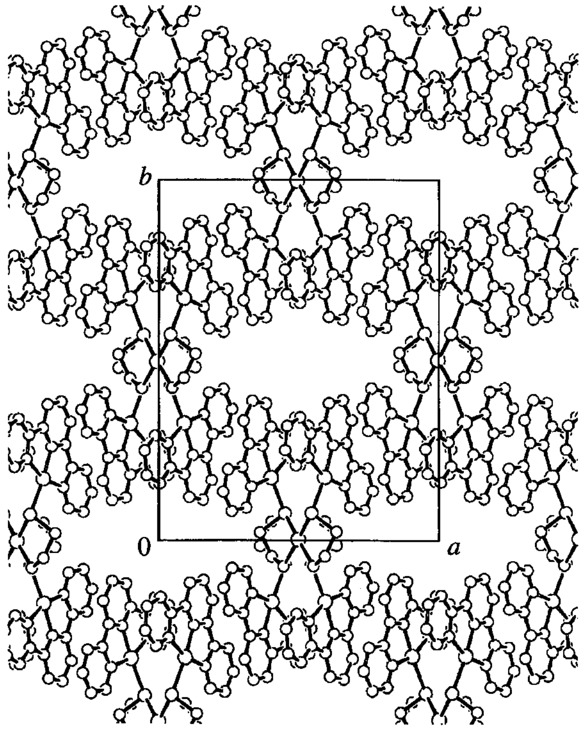

Fig. 6. Projection of crystal packing for [{Pd(terpy)}$_2${Pd(aet)$_2$}](SiF$_6$)$_2$·6H$_2$O (4) viewed along *c* axis.

structure with an alternating coplanar stacking arrangement, which is contrasted to the intermolecular stacking arrangement of **3**. Namely, one {Pd(terpy)} moiety in one complex cation is overlapped with one {Pd(terpy)} moiety in another complex cation. Furthermore, another {Pd(terpy)} moiety in one complex cation approaches to one {Pd(terpy)} moiety in the other complex cation. Therefore, the interplane distances (av 3.417 Å) and angles (av 0.21°) between the neighboring {Pd(terpy)} moieties are also within the range of the π–π stacking contact.[3]

Diffuse Reflection Spectra. The diffuse reflection spectra of **1**—**4** are shown in Fig. 7, and the data are summarized in Table 3. [{Pd(terpy)}$_2${Pd(aet)$_2$}](PF$_6$)$_4$·2CH$_3$CN (**1**) exhibits two peaks at 27.03 and 28.57×10^3 cm^{-1}, and two shoulders around 24.9 and 32.5×10^3 cm^{-1}. Among these bands, the 24.9×10^3 cm^{-1} one is characteristic of the *S*-bridged Pd(II) complex with an intramolecular stacking arrangement.[20] On the other hand, the 32.5×10^3 cm^{-1} band is assigned as a π–π* transition localized in a terpy skeleton. The bands at 27.03 and 28.57×10^3 cm^{-1} are considered to be transitions concerned with Pd atoms or terpy. In the case of [{Pd(terpy)}$_2${Pd(aet)$_2$}](BF$_4$)$_4$·0.5H$_2$O (**2**), the bands corresponding to the above 24.9, 27.03, 28.57, and 32.5×10^3 cm^{-1} ones are located at 23.7, 26.92, 28.1, and 33.44×10^3 cm^{-1}. There is considerable difference (ca. 1.2×10^3 cm^{-1}) in the transition energies between the highest energy bands of **1** and **2**. This is reflected by the differences in the intramolecular stacking modes of these complexes. Although the above four bands are observed in each case of [{Pd(terpy)}$_2${Pd(aet)$_2$}](BF$_4$)$_4$ (**3**) and [{Pd(terpy)}$_2${Pd(aet)$_2$}](SiF$_6$)$_2$·6H$_2$O (**4**), one additional shoulder is located at a lower energy side than 20×10^3 cm^{-1}. Since these bands are found only for polymeric **3** and **4**, but not for monomeric

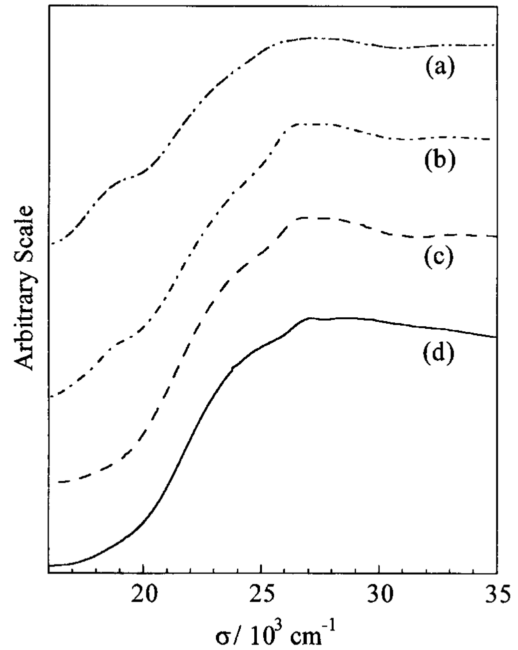

Fig. 7. Diffuse reflection spectra of (a) [{Pd(terpy)}$_2${Pd(aet)$_2$}](SiF$_6$)$_2$·6H$_2$O (**4**), (b) [{Pd(terpy)}$_2${Pd(aet)$_2$}](BF$_4$)$_4$ (**3**), (c) [{Pd(terpy)}$_2${Pd(aet)$_2$}](BF$_4$)$_4$·0.5H$_2$O (**2**), and (d) [{Pd(terpy)}$_2${Pd(aet)$_2$}](PF$_6$)$_4$·2CH$_3$CN (**1**).

Table 3. Diffuse Reflection Spectral Data of [{Pd(terpy)}$_2${Pd(aet)$_2$}](PF$_6$)$_4$·2CH$_3$CN (**1**), [{Pd(terpy)}$_2${Pd(aet)$_2$}](BF$_4$)$_4$·0.5H$_2$O (**2**), [{Pd(terpy)}$_2${Pd(aet)$_2$}](BF$_4$)$_4$ (**3**), and [{Pd(terpy)}$_2${Pd(aet)$_2$}](SiF$_6$)$_2$·6H$_2$O (**4**)

	Reflection maxima σ / 10^3 cm^{-1}
[{Pd(terpy)}$_2${Pd(aet)$_2$}](PF$_6$)$_4$·2CH$_3$CN (**1**)	24.9^{sh}, 27.03, 28.57, 32.5^{sh}
[{Pd(terpy)}$_2${Pd(aet)$_2$}](BF$_4$)$_4$·0.5H$_2$O (**2**)	23.7^{sh}, 26.92, 28.1^{sh}, 33.44
[{Pd(terpy)}$_2${Pd(aet)$_2$}](BF$_4$)$_4$ (**3**)	19.0^{sh}, 23.8^{sh}, 26.74, 27.70, 32,79
[{Pd(terpy)}$_2${Pd(aet)$_2$}](SiF$_6$)$_2$·6H$_2$O (**4**)	18.9^{sh}, 23.5^{sh}, 27.17, 28.3^{sh}, 33.00

The sh label denotes a shoulder.

1 and **2**, they are regarded to originate in the intermolecular stacking structures. Reflecting the differences between the intermolecular stacking modes of **3** and **4**, furthermore, the transition energies of the bands are different from each other.

This work was partially supported by a Grant-in-Aid for Scientific Research No. 11640555 from the Ministry of Education, Science, Sports and Culture.

References

1 E. Bielli, P. M. Gidney, R. D. Gillard, and B. T. Heaton, *J. Chem. Soc., Dalton Trans.*, **1974**, 2133.

2 W. I. Sundquist and S. J. Lippard, *Coord. Chem. Rev.*, **100**, 293 (1990).

3 W. B. Connick, R. E. Marsh, W. P. Schaefer, and H. B. Gray, *Inorg. Chem.*, **36**, 913 (1997).

4 K. R. Koch, C. Sacht, and C. Lawrence, *J. Chem. Soc., Dalton Trans.*, **1998**, 689.

5 Y. Yamada, M. Uchida, Y. Miyashita, K. Fujisawa, T. Konno, and K. Okamoto, *Bull. Chem. Soc. Jpn.*, **73**, 913 (2000).

6 S. S. Kamath, V. Uma, and T. S. Srivastava, *Inorg. Chim. Acta*, **161**, 49 (1989).

7 V. H. Houlding and V. M. Miskowski, *Coord. Chem. Rev.*, **111**, 145 (1991).

8 H. Yip, H. Lin, K. Cheung, C. Che, and Y. Wang, *Inorg. Chem.*, **33**, 1644 (1994).

9 B. Tzeng, W. Fu, C. Che, H. Chao, K. Cheung, and S. Peng, *J. Chem. Soc., Dalton Trans.*, **1999**, 1017.

10 S. Lai, T. Cheung, M. C. W. Chan, K. Cheung, S. Peng, and C. Che, *Inorg. Chem.*, **39**, 255 (2000).

11 P. M. Kiernan and A. Ludi, *J. Chem. Soc., Dalton Trans.*, **1978**, 1127.

12 M. Cusumano, M. L. D. Pietro, A. Giannetto, F. Nicolò, and E. Rotondo, *Inorg. Chem.*, **37**, 563 (1998).

13 A. Gelling, K. G. Orrell, A. G. Osborne, and V. Šik, *J. Chem. Soc., Dalton Trans.*, **1998**, 937.

14 K. Okamoto, Y. Yoshinari, Y. Yamada, N. Sakagami, and T. Konno, *Bull. Chem. Soc. Jpn.*, **71**, 1363 (1998).

15 V. F. Sutclifee and G. B. Young, *Polyhedron*, **3**, 87 (1984).

16 F. L. Wimmer and S. Wimmer, *Inorg. Chim. Acta*, **149**, 1 (1988)

17 S. Wimmer, P. Castan, F. L. Wimmer, and N. P. Johnson, *J. Chem. Soc., Dalton Trans.*, **1989**, 403.

18 W. Paw, W. B. Connick, and R. Eisenberg, *Inorg. Chem.*, **37**, 3919 (1998).

19 B. Oskui, M. Mintert, and W. S. Sheldrick, *Inorg. Chim. Acta*, **287**, 72 (1999).

20 Y. Yamada and K. Okamoto, *Chem. Lett.*, **1999**, 315.

21 J. C. Dewan, S. J. Lippard, and W. R. Bauer, *J. Am. Chem. Soc.*, **102**, 858 (1980).

22 G. Anderegg and H. Wanner, *Inorg. Chim. Acta*, **113**, 101 (1986).

23 D. C. Jicha and D. H. Busch, *Inorg. Chem.*, **1**, 872 (1962).

24 D. C. Jicha and D. H. Busch, *Inorg. Chem.*, **1**, 878 (1962).

25 "teXsan. Molecular Structure Corporation. Single Crystal Structure Analysis Software. Version 1.9," MSC, 3200 Research Forest Drive, The Woodlands, TX77381, USA (1998).

26 Lists of final atomic coordinates and equivalent isotropic thermal parameters for hydrogen atoms, anisotropic thermal parameters for non-hydrogen atoms, and bond distances and angles are deposited as Document No. 73053 at the Office of the Editor of Bull. Chem. Soc. Jpn.